Received: 12 September 2022 | Revised: 24 October 2022 | Accepted: 20 November 2022

DOI: 10.1002/we.2797

RESEARCH ARTICLE

WILEY

A passively self-adjusting floating wind farm layout to increase the annual energy production

Mohammad Youssef Mahfouz | Po-Wen Cheng

Stuttgart Wind Energy (SWE), University of Stuttgart, Allmandring 5B, Stuttgart, 70569, Germany

Correspondence
Mohammad Youssef Mahfouz, Stuttgart Wind Energy (SWE), University of Stuttgart, Allmandring 5B, 70569 Stuttgart, Germany.
Email: mahfouz@ifb.uni-stuttgart.de

Funding information
Horizon 2020 research and innovation program under grant agreement no. 815083 (COREWIND).

Abstract

Wake losses inside a wind farm occur due to the aerodynamic interactions when a downwind turbine is in the wake of upwind turbines. The ability of floating offshore wind turbines (FOWTs) to relocate their positions in the horizontal plane introduces an opportunity to decrease the wake losses in a floating wind farm (FWF). Our goal is to use this ability to passively move the downwind FOWT out of the wake of upwind ones. Since the mooring system (MS) attached to a FOWT is responsible for its station keeping, the horizontal motions of the FOWT depend on the MS design. Hence, if we can design the MS to passively move the FOWT out of the wake, we can increase the FWF annual energy production (AEP). In this paper, we investigate if we can benefit from relocating FOWTs in a FWF and increase its AEP. In addition, we present a novel approach that considers the ability of a FOWT to relocate its position as a new degree of freedom (DoF) in the FWF layout design. This means we will have a self-adjusting wind farm layout where the FOWTs passively re-arrange themselves depending on the wind direction and the wind speed. Consequently, we will have a slightly different wind farm layout for every wind direction and every wind speed. To achieve this layout, we include the MS design as part of the FWF's layout design. In a self-adjusting FWF layout, each FOWT is attached to a customized MS design allowing it to relocate its position in the best way possible according to the wind direction, to increase the overall AEP of the wind farm. The results of one case study show that the novel approach can increase the FWF's AEP by 1.6% when compared with a current state of the art optimized floating wind farm layout. Finally, we implemented our method as an open-source python tool to be used and enhanced further within the wind energy community.

KEYWORDS
floating wind energy, floating wind farms, mooring systems, wake losses, wind farm layout optimization

1 | INTRODUCTION

As a wind turbine extracts energy from the free flow wind field, the wind speed behind the turbine decreases and the turbulence increases. When this lower energy and more turbulent wind field hits a downwind turbine, wake losses occur as the downwind turbine extracts less energy than the upwind one. Moreover, as the downwind flow is more turbulent, the fatigue loads on the downwind turbine are higher.[1,2] These energy losses increase the levelized cost of energy (LCOE) of the wind farm. Therefore, to decrease the LCOE of the wind farm, different optimization objectives can be chosen to target each of the different drivers of the farm's LCOE. A common optimization objective is to increase the AEP of the farm, and other optimization objectives are to increase the power density of the wind farm or to decrease the electrical cables' length used in the farm.[3] In addition, we can use multi-disciplinary analysis and optimization (MDAO) to consider the interactions between the different components of a wind farm design and decrease the farm's LCOE.[4] However, none of these techniques eliminates the wake losses that remain significant. Additionally, none of the current wind farm design techniques considers the fact that FOWTs are not fixed to the ground and are allowed to move in the horizontal plane. To the best of our knowledge, there are no available tools or methods that investigate the effect of the horizontal motions of FOWTs on a FWF performance.

FOWTs differ from fixed bottom turbines as they are not fixed to the ground, but attached to a MS for station keeping. The FOWT's displacements in the horizontal plane are defined by the design of the MS attached to it. The controlled area where the MS allows the FOWT to drift around is called the watch circle. Following the oil and gas industry, the current state of the art MS designs only allows minimum displacements for the FOWT, that is, a small watch circle. However, the ability of a FOWT to move in the horizontal plane presents an opportunity to reduce the wake losses in a FWF. If we can design the MS allowing a downwind FOWT to displace in the crosswind direction, we can move this FOWT out of the wake and decrease the wake losses. But the question is, can we use the ability of a FOWT to passively relocate its position in the horizontal plane to increase a FWF's AEP?

Fleming et al[5] aligned two turbines behind each other facing the wind and moved the downwind turbine in the crosswind direction. The study shows that the energy gain becomes visible when the downwind turbine is displaced in the crosswind direction by 20% of the turbine's rotor diameter (*D*). The energy gain reaches 41% if the downwind turbine is displaced by 1*D*. The study shows the potential of relocating downwind FOWT, but it does not discuss how the FOWT can achieve crosswind displacements. Additionally, the study does not discuss the effect of relocating the turbines or of changing the wind direction on a wind farm level. Kheirabadi and Nagamune[6,7] applied a yaw and induction-based controller to actively relocate the FOWTs' positions. The results show that even with an active controller, the FOWT ability to relocate its position is governed by the MS design and its watch circle. Rodrigues et al[8] introduced an optimization framework to change the positions of the wind turbines according to the wind direction. However, the motions are achieved by actively controlling the position of the FOWT relative to the anchors using pulleys. To the best of our knowledge, this work is the first study that aims to relocate the FOWTs passively, that is, without actuators or active controllers, only using the MS design to increase the FWF's AEP.

In this paper, we investigate the benefit of passively relocating FOWTs on the AEP of a FWF. Additionally, we present a methodology that includes the MS design as part of the FWF layout design, where each FOWT is attached to a customized MS to increase the overall FWF's AEP. Finally, the method is implemented as an open-source python-based tool to be used and enhanced further by the wind energy community. The aim of the methodology introduced here is not to find a global optimum FWF design. Our aim is to demonstrate that it is beneficial to include the FOWT's horizontal motions as a design variable while designing the farm's layout. Moreover, we are using AEP as an optimization objective for the wind farm layout, without calculating the LCOE of the FWF as this is out of scope for the present study. The paper is structured as follows: First, we present the suggested methodology for a FWF dynamic layout design, and then we use a case study to calculate the gain in a FWF's AEP; finally, we summarize our work and present our conclusion and pointers for future research.

2 | METHODOLOGY

In this section, we will present in detail the developed method to design a FWF layout. Our goal is to have a FWF layout that changes with the wind direction to reduce the wake losses within the farm and increase its AEP. We start by summarizing our method in Figure 1, the inputs needed to start the process are a baseline layout of a wind farm, the wind rose, the FOWT's parameters including aerodynamic properties as well as hydrostatic properties, and finally the MS design parameters. As we see in Figure 1, the method has six main steps to design a dynamic FWF layout. To decrease the computation time, the first and second steps are done in parallel while doing the third and fourth steps. In the following subsections, we will present the six main steps in detail. The method is implemented as an open-source python-based tool.[9]

Throughout this section, we are building on and benefiting from the knowledge we gained in our previous work presented in Mahfouz et al.[10] First, we use the same methods to create the MS database in Sections 2.3, and 2.4. Afterwards, we use the knowledge we gained on how the line headings affects the FOWT motions in Section 2.5.1. In Mahfouz et al,[10] we showed that mooring systems with the same headings will have the same watch circle shape. The other design parameter can be used to tune the magnitude of the FOWT's displacement without affecting the overall watch circle shape.

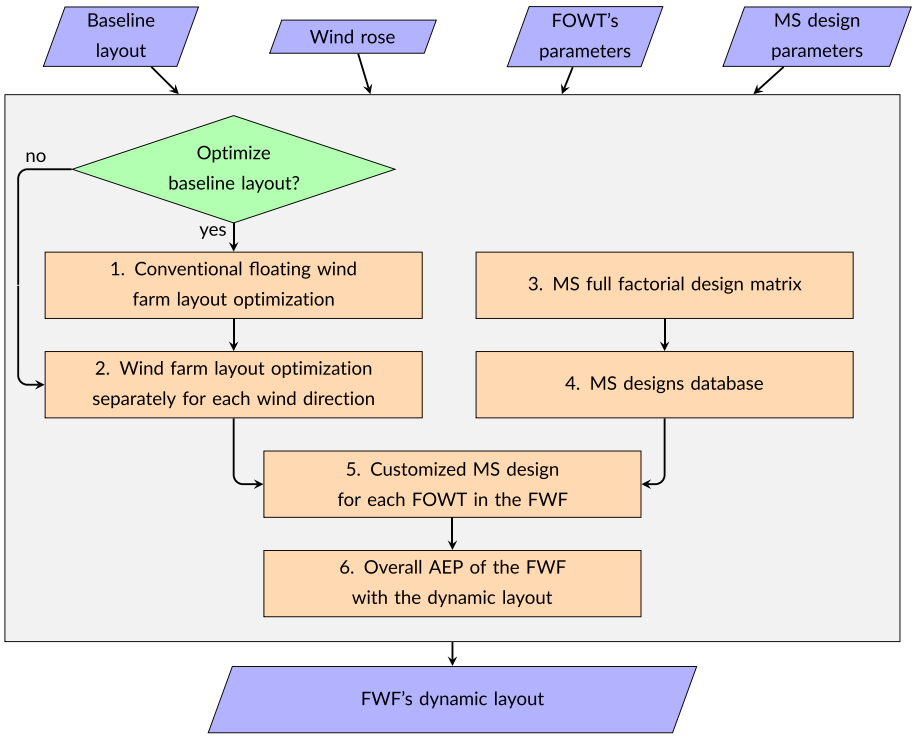

FIGURE 1 Methodology for FWF dynamic layout design

2.1 | Conventional floating wind farm layout optimization

The first step is optional depending on the decision of the user and the input baseline wind farm layout. If the given baseline layout is already optimized or if it is the layout of an existing wind farm to be used as a case study, then this step is not needed. However, if the baseline layout requires optimization, this step is necessary as it affects the entire process that follows. The reason is that we will use the layout produced at the end of this step as a reference layout and its AEP will be the reference AEP value (AEP_0). If AEP_0 is not an optimum value, we can get a higher gain by using a dynamic FWF layout, than what we will achieve if AEP_0 is the optimum value. This will make it hard to assess if we can benefit from relocating the FOWT. Therefore, to conclude whether it is beneficial to implement a dynamic FWF layout, we need to be sure that our layout after this step is as close as possible to the global optimum solution. Throughout this paper, we refer to this optimized layout as optimum wind farm layout (OWFL).

For wind farm layout optimization, we need a wake model and an optimization algorithm. We used the open-source tool FLORIS v2.4,[11] to supply the wake model. Moreover, we used the pyOptSparse framework[12] for wind farm layout optimization since it includes different optimization algorithms to choose from. The inputs needed for this step are the baseline layout, the wind rose, and the turbine's power and thrust coefficients. Finally, to decrease the computational costs, we assume the wind speed is constant for all wind directions and equal to the turbine's rated wind speed as postulated by Baker et al[13] and Thomas et al.[14] In this step, the FOWTs in the FWF are assumed to be stationary following the current state of the art for FWF layout design.

2.2 | Targeted FWF layout

After we obtained the OWFL, we start optimizing it for each wind direction separately. This means we will have a different FWF layout for each wind direction. To ensure that the optimum layouts for different wind directions are not totally new layouts when compared with the OWFL, we added two constraints for this optimization.

- The turbines are only allowed to move in the crosswind direction.
- The crosswind displacement cannot be higher than a user defined value.

These constraints ensure that the layout for each wind direction is only a slightly different layout, when compared to the OWFL. In this step, we also assume the wind speed is constant for all wind directions and equal to the turbine's rated wind speed. Throughout the paper, we will refer to the layouts we produce in this step as targeted FWF layouts. From these layouts, we obtain the crosswind displacements each FOWT in the farm makes for each wind direction. We store these targeted displacements as a $(wdir \times t)$ matrix, where *wdir* is the number of wind directions and t is the number of FOWT in the FWF. Through the rest of this work, we refer to this matrix as $\Delta \boldsymbol{X_{tr}}$. The targeted crosswind displacement of a single FOWT is a vector with length *wdir* (i.e., a single column from the $\Delta \boldsymbol{X_{tr}}$ matrix), and we refer to it as ΔX_{tr}.

2.3 | Mooring systems full factorial design matrix

In this step, we want to create a full factorial design matrix to be the design space for the MS designs. In order to create this full factorial design matrix, we used the same method we presented in Mahfouz et al.[10] The MS design parameters were divided into two types of parameter: first, constant parameters that have fixed values for all MS designs and, second, permutable design parameters where every combination of these parameters is different for each MS design.

The constant design parameters include the number of mooring lines, the water depth, and the line material. Additionally, the MS must have a catenary shape, with no vertical forces on the anchors. The permutable parameters include the line headings, the line diameters, the anchor radii R, and the lines length L. The lines' length is a function of the anchor radii R and the water depth as shown in Equation (1). The coefficient β ensures that the line is always between the minimum L_{min} and maximum L_{max} allowable values.

$$L_{min} = \sqrt{depth^2 + R^2} \tag{1a}$$

$$L_{max} = depth + R \tag{1b}$$

$$L = L_{min} + \beta(L_{max} - L_{min}) \qquad 0 \le \beta \le 1 \tag{1c}$$

2.4 | Mooring systems database

After the MS factorial design matrix is created, we create the MS database as shown in Figure 2, following the method we presented in Mahfouz et al.[10] First, we find the static equilibrium position vector of the FOWT (X_0) when attached to the MS design in the absence of any external forces. Afterwards, we apply the aerodynamic thrust force at the rated wind speed and calculate the new equilibrium position vector of the FOWT (X_1) at each wind direction. Then we check if the position vector satisfies the user defined constraints. If all constraints are satisfied, we save the MS with the position vectors X_0, and X_1 to our database. Finally, we repeat these steps until we iterate over all MS designs in our full factorial design matrix. Afterwards, we calculate the displacements of the FOWT when the aerodynamic force is applied ($\Delta X = X_1 - X_0$). Then we decompose the FOWT's displacements into crosswind (ΔX_p) and in-wind (ΔX_w) displacements. For each MS, ΔX_p is a vector, which has its crosswind displacements at each wind direction; hence, the length of ΔX_p is equal to the number of wind directions.

We use the aerodynamic thrust force at rated wind speed for two reasons. First, there are no energy losses due to wakes above the rated wind speeds as the FOWTs will always produce the rated power. Another reason is that the thrust has the highest value at rated wind speed, so it will cause the biggest displacements and the highest forces on our MS. Therefore, if the MS designs fulfill the user defined constraints at rated thrust, we can expect the same at all other wind speeds. Moreover, it will be time consuming to recalculate the database at all wind speeds between cut in and cut out wind velocities, hence for this step it is enough to use the rated value. In addition, we neglect the effect of the mean wave forces on the FOWT's ability to relocate, because they are small when compared with the aerodynamic forces.

2.5 | Customized MS design

The goal of this step is to find the MS design to attach to each FOWT in the FWF to increase the farm's energy production. The highest gain in the FWF's energy will happen if we find a MS design where $\Delta X_p = \Delta X_{tr}$ for each FOWT in the farm, but this is not realistic as we will never find MS designs that can fulfill the targeted layout for all FOWTs in the FWF for all wind directions. This is explained in Figure 3, which gives a theoretical example for how ΔX_p and ΔX_{tr} look, and shows that ΔX_p and ΔX_{tr} cannot be equal for all wind directions. On the other hand, if we choose the MS design for each FOWT in the FWF that achieves the minimum difference ($min(\Delta X_p - \Delta X_{tr})$), this will not guarantee that we end up with

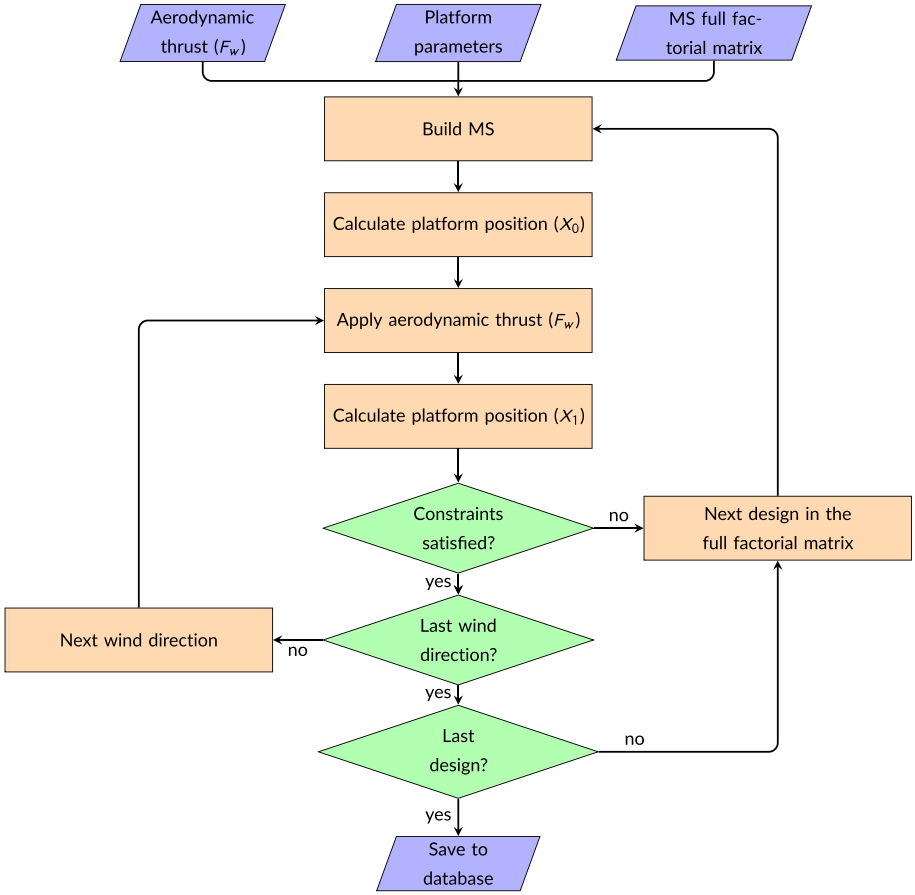

FIGURE 2 Creating MS database

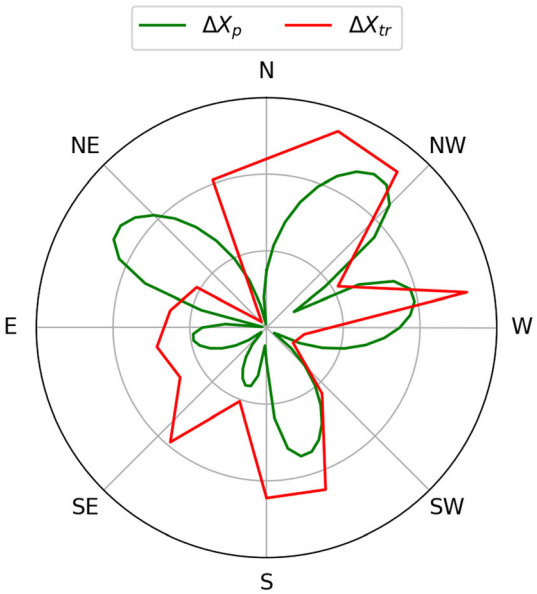

FIGURE 3 A comparison between the crosswind displacement of a MS (ΔX_p) and the targeted crosswind displacement (ΔX_{tr})

an increase in energy production for the FWF. Because if we displace a FOWT opposite to the targeted displacements in a wind direction, this will lead to higher wake loses and hence less energy production, since our goal is to find a customized MS for each FOWT to achieve the highest overall energy production of the FWF. Therefore, we want to find a MS design for each FOWT where $\Delta X_p = \Delta X_{tr}$ only for some wind directions to

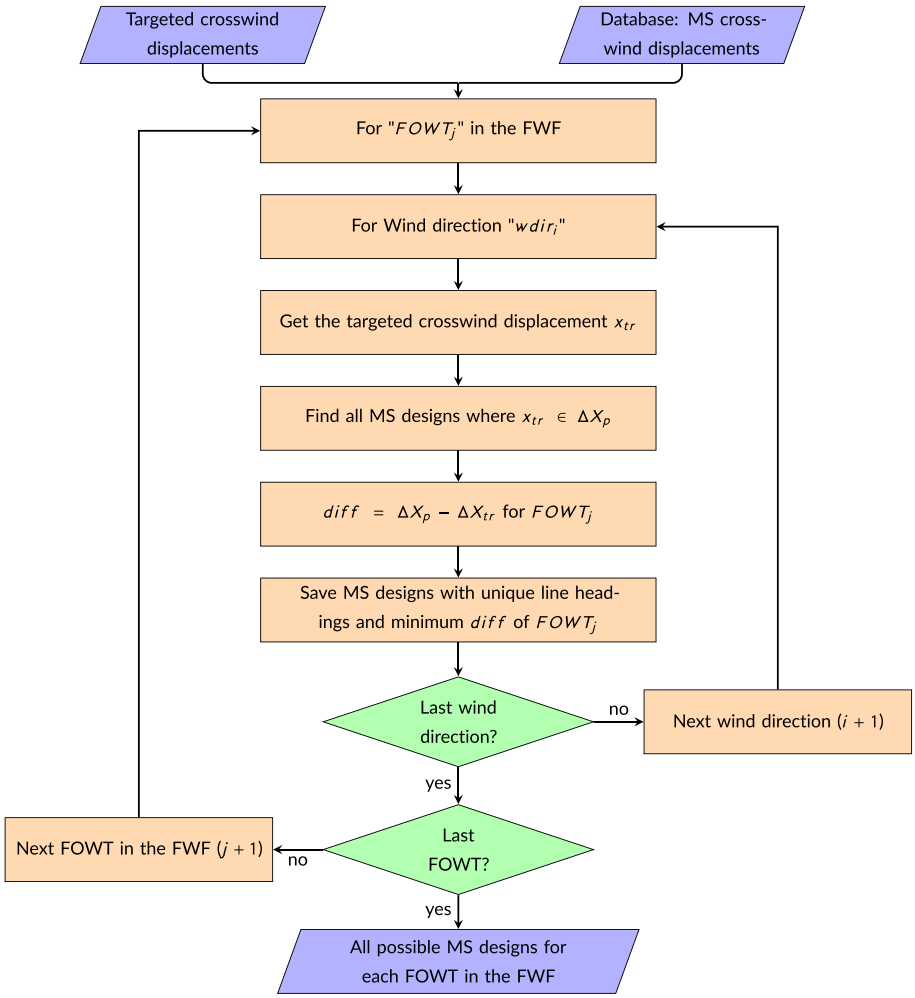

FIGURE 4 Finding all possible MS designs that can be attached to each FOWT in the FWF

achieve the targeted energy gain for these directions, without causing higher losses in the other wind directions where $\Delta X_p \neq \Delta X_{tr}$. We will achieve this goal through two steps: First, we will find all the possible MS designs that can be attached to each FOWT as shown in Figure 4. Afterwards, we will iterate over this design space of possible MS designs to find a single MS design for each FOWT as shown in Figure 5. This will give us a FWF dynamic layout that produces higher energy, when compared with the OWFL.

2.5.1 | Possible MS designs for each FOWT

Our design space for MS designs is the database created in Section 2.4, but this database includes thousands of possible MS designs. So, we cannot use brute force optimization and attach each MS design in our database to each FOWT in the FWF as this will be computationally inefficient, for example, if we assume that we have a small FWF with only four FOWTs and a database that only has 10^3 MS designs. For this assumption, if we want to try every possible combination of MS designs for the four FOWTs, we have 10^{12} possibilities; hence, we need to calculate the energy production of this small FWF 10^{12} times to be able to find the optimum MS design for each FOWT. Therefore, even for a small FWF, this is computationally expensive.

This step narrows down our MS design space to a subset of the MS database. As the targeted displacement of each FOWT in the FWF is different, we find a smaller MS design space for each FOWT separately. To achieve this goal, we follow the approach shown in Figure 4. First, we start with the selection of a single $FOWT_j$ from the t FOWTs in the FWF. Then we choose a wind direction $wdir_i$ from the $wdir$ wind directions in the wind rose. Afterwards, we find the targeted crosswind displacement the $FOWT_j$ needs to achieve at $wdir_i$. Since we are only looking at one wind direction ($wdir_i$) and one FOWT ($FOWT_j$), this is only one value from the ΔX_{tr} vector, and we refer to this value as Δx_{tr}. Afterwards, we find all MS designs whose crosswind displacement vectors ΔX_p contain x_{tr}. Then we use these MS designs to calculate the difference ($diff$) between

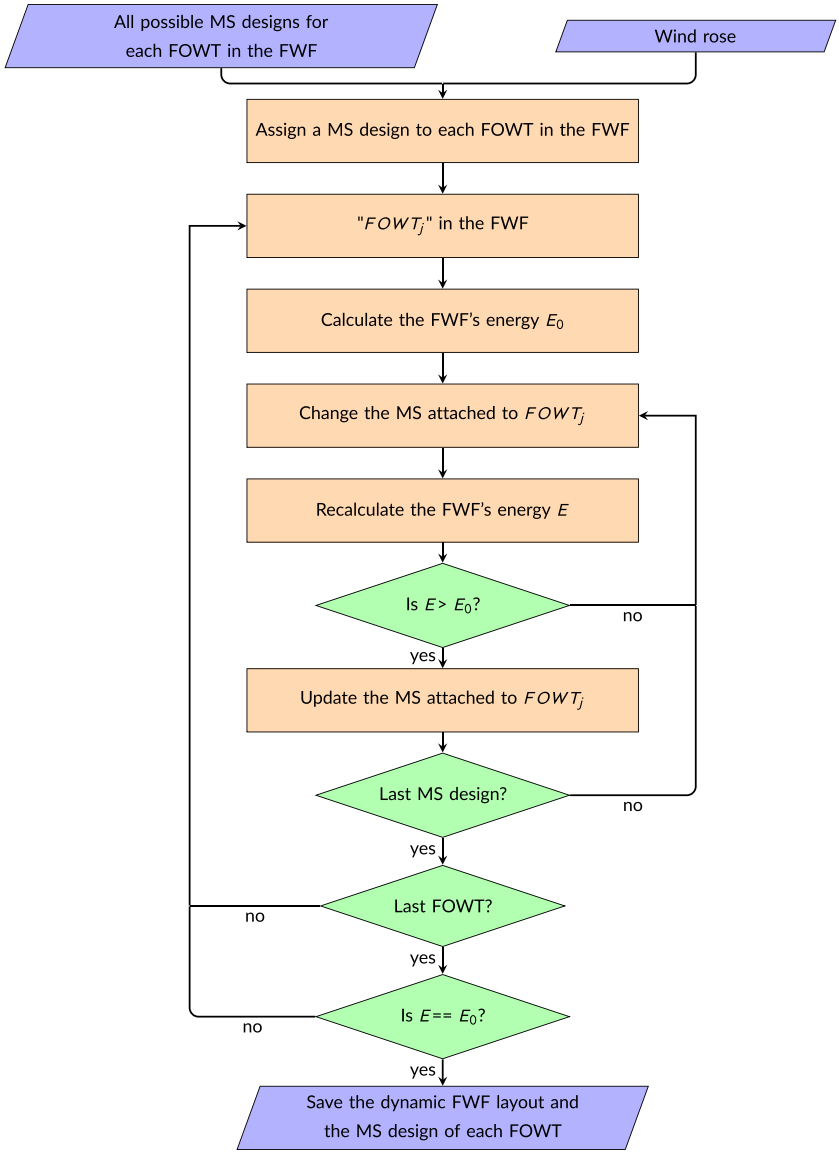

FIGURE 5 Customizing the MS design attached to each FOWT

the crosswind displacements vector of each of these MS designs ΔX_p and the targeted crosswind displacements vector ΔX_{tr} of $FOWT_j$ as in Equation (2).

$$diff = \Sigma|\Delta X_{tr} - \Delta X_p| \tag{2}$$

To decrease the design space further, we will use the *diff* value and the line headings from the MS design parameters. We know from Mahfouz et al[10] that all MS designs with the same line headings have the same watch circle shape. All the other MS design parameters can only tune the watch circle to decrease or increase the displacements (i.e., make the watch circle bigger or smaller). When MS designs share the same watch circle shape, we can predict that if one of them causes an energy gain in one wind direction, all other MS with the same watch circle shape will cause energy gain at this wind direction. However, each of these designs with the same watch circle shape will lead to a different value of energy gain. The MS design causing the highest gain will be the design with the crosswind displacement closest to the targeted displacements ($min(diff)$). Similarly, if one of the MS designs with the same watch circle shape causes energy loss in one wind direction, all the other designs with the same watch circle shape will also cause energy loss. The MS design causing the highest loss will be the design with the crosswind displacement furthest to the targeted displacements ($max(diff)$). Based on this, we can filter the MS designs to have only one MS design from

each line headings value. To decide which design to choose for each line headings value, we will use the *diff* values we calculated earlier. For all the MS designs sharing the same headings, we will choose only the design with the minimum *diff* value.

Finally, we will iterate over all wind directions to have the new MS design space for $FOWT_j$. Then we repeat the entire process for all other FOWTs in the FWF. We believe that depending on the MS design headings and the *diff* values to find a subset of the MS database, does not lead to the global optimum MS design for each FOWT. However, as our goal is not to find the global optimum solution, but to check whether relocating FOWT can increase a FWF energy production, this is a robust and reliable approach.

This process will decrease our design space compared to using the full database as a design space. For example, if our database has 10 unique line headings, and 16 wind directions, we end up with a design space made of 160 possible MS designs instead of the full database of 10^3 possible MS designs. If we use brute force for a FWF of four turbines, we have approximately $6.5 * 10^8$ possibilities for the FWF layout instead of 10^{12} possibilities. However, $6.5 * 10^8$ FWF layout possibilities are still computationally expensive. Therefore, we will decrease the FWF layout possibilities further in the following section.

2.5.2 | MS design attached to each FOWT

Figure 5 explains the method we follow to choose one MS for each FOWT in the farm. To avoid iterating over every possibility, first we randomly assign a MS to each FOWT in the farm from the MS designs space. Afterwards, we calculate the FWF energy production (E_0). Then for only one FOWT ($FOWT_j$), we iterate over all its possible MS designs and attach to it the design, which leads to the highest energy production of the FWF (E). We repeat this process for all FOWT in the FWF till the energy production of the farm converges. Finally, we save the MS attached to each FOWT. This process will cut down the computational time needed to find the customized MS designs for each of the FOWTs. For example, if we have 160 possible MS designs for each FOWT in a four-turbine FWF, then one iteration means we have $160 * 4$ iterations. Assuming we will need 10 iterations till the FWF energy converges, we end up with 6400 iterations instead of the $6.5 * 10^8$ iterations we would need if we just used brute force optimization with all possible combinations of MS designs.

2.6 | Calculate the overall AEP of the FWF with the dynamic layout

The last step in our method is to calculate the total FWF's AEP to conclude whether we benefit from relocating the FOWT and to quantify the gain in the FWF's AEP. Until this point, we assumed that the wind speed is constant for all wind directions and is equal to the turbine's rated wind speed. Therefore, in this step, we want to calculate the FWF's AEP considering the entire range of wind speeds. To do this, we need to calculate the watch circle of each MS design coupled to each FOWT in the farm for all wind speeds between cut in and cut out. The watch circle changes with the change of the aerodynamic thrust, and since the MS' stiffness is nonlinear, we cannot predict the watch circle at different wind speeds. This means that the layout of a FWF will be slightly different for each wind speed and each wind direction. In this step, we only calculate the watch circles of the chosen customized MS designs (from Section 2.5) attached to the FOWTs in the FWF and will not calculate the entire MS database at each wind velocity. After calculating the different watch circles at different wind velocities, we calculate the overall AEP of the FWF and compare it to the reference AEP_0.

3 | RESULTS

3.1 | Introducing a general case study

To apply the methods, we presented earlier we need to define a general case study as proof of concept, so we decided to follow case study one from the international energy agency (IEA) Task 37 and presented in the work of Baker et al.[13] We created a FWF layout made of two concentric circles including 19 turbines to be used as a baseline layout as presented in Figure 6. The spacing between any two neighboring turbines is fixed to 5*D*. For the wind turbines, we used the 15MW IEA reference wind tribune coupled to the Activefloat platform as presented by Mahfouz et al.[15] The wind rose used was taken from the IEA Task 37[13] and shown in Figure 6. For the following sections, the wind speed is constant for all wind directions and equal to 10 m/s, except for Section 3.7, where we calculate the overall FWF's AEP, and use the full wind rose. The rated wind speed of the IEA 15 MW is approximately 10.5 m/s, which is close to the wind speed used in the calculations. The wake model used throughout this paper is the Gaussian wake model implemented in FLORIS v2.4. The model calculates the velocity deficit as presented by Abkar and Porté-Agel[16] and Bastankhah and Porté-Agel.[17] Additionally, the wake added turbulence is implemented following the work of Crespo and Hernández.[18] We used the default calibrated Gaussian model parameters from NREL.[11]

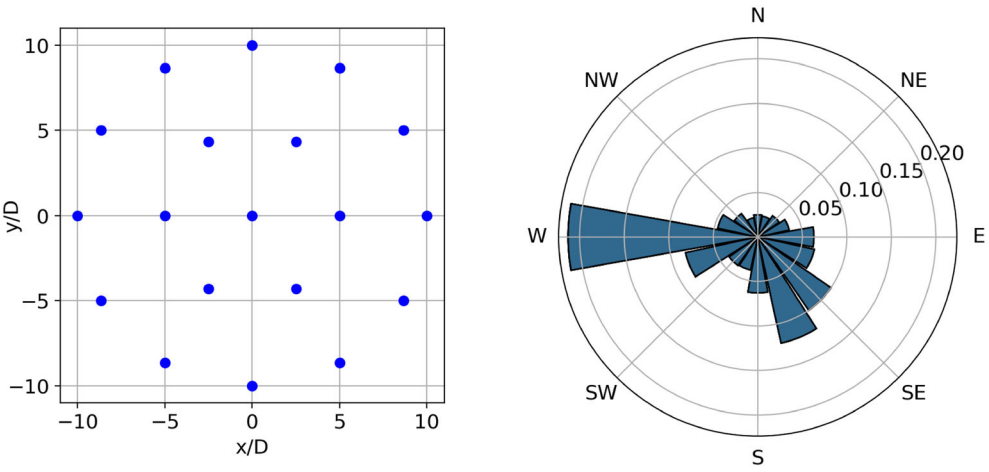

FIGURE 6 Wind rose with constant wind speed (right) and baseline wind farm layout (left)

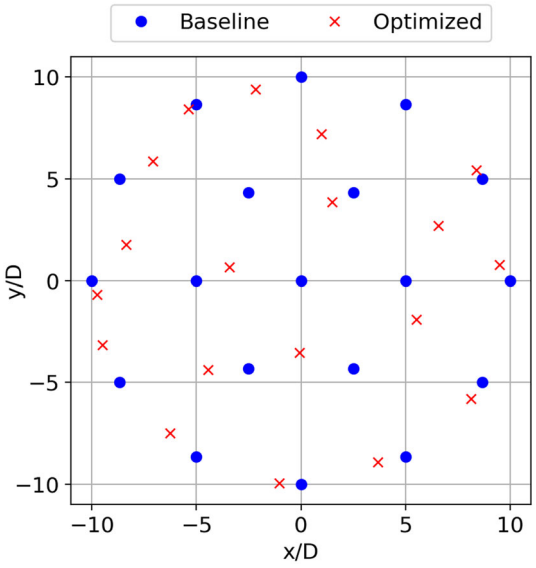

FIGURE 7 Baseline layout optimization

3.2 | Conventional state of the art wind farm layout optimization

For the baseline layout optimization, we used the gradient based optimization algorithm SNOPT v7.7,[19] as it led to the wind farm layout with the highest energy production in Baker et al.[13] Our optimization objective was maximizing the farm's energy production, and we had two optimization constraints. First, the minimum distance between any two turbines could not be less than 2*D*. Second, no turbine was allowed to exist outside the wind farm's boundaries. In SNOPT, the optimality tolerance was set to $5 * 10^{-5}$, the feasibility tolerance was set to 10^{-6}, and the scale option was set to 2. The wind rose in Figure 6 was used during this step. The output of this optimization produced the OWFL shown in Figure 7. The OWFL can produce 6.4% more energy when compared to the baseline layout at constant wind speed of 10 m/s for all wind directions.

3.3 | Targeted FWF layout

In order to reach our targeted dynamic FWF layout, we optimized the FWF separately for each wind direction. We again used the gradient-based optimization algorithm SNOPT, and the optimization goal was to increase the energy production. However, our optimization constraints were

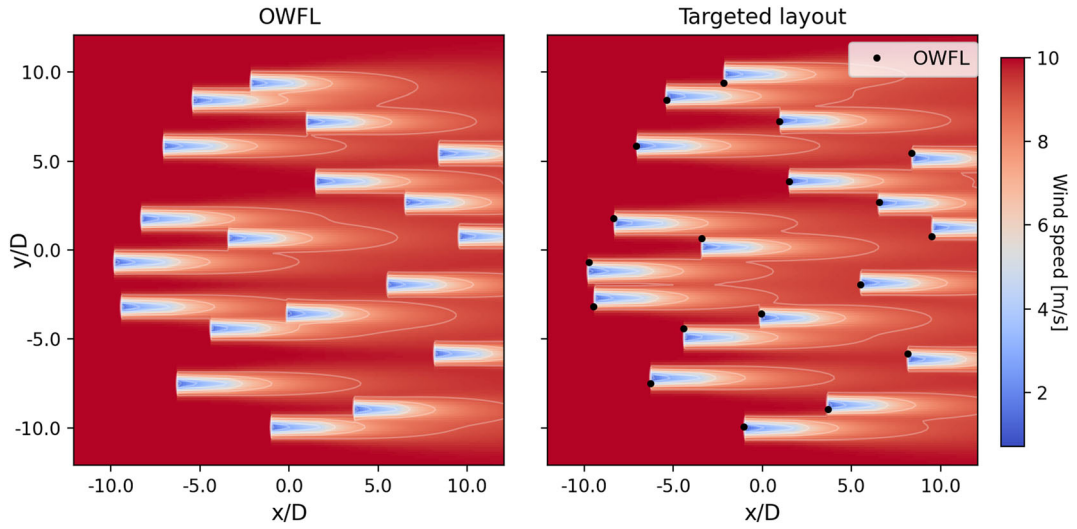

FIGURE 8 The OWFL and targeted FWF layouts at the main wind direction at 10 m/s

different. First, we only allowed the turbines to displace in the crosswind direction. Second, we only allowed a maximum displacement of 0.5*D*. We chose the value of 0.5*D* such that if two turbines were aligned behind each other and they both displaced in crosswind direction, the overall relative displacement was 1*D*. In general, this constraint depends on the minimum allowable distance constraint defined during the baseline optimization in Section 3.2. Since our constraint in Section 3.2 was defined as 2*D*, our maximum allowable crosswind displacement cannot be more than 0.5*D*. If two turbines in the OWFL are next to each other and separated by the minimum distance of 2*D*, and in the targeted layout design, they both move 0.5*D* in the crosswind direction toward each other, and then the distance between these two turbines will decrease to 1*D*. If the allowable crosswind displacement increases, this could decrease distance between two turbines to less than 1*D*, which is not realistic as in this case the blades of the two turbines will hit each other. Additionally, in this step, we did not add a constraint to force the FOWTs to stay within the FWF boundaries, because the increase in the FWF's area is small and has no effect on the energy gain. Increasing the FWF boundary diameter from 20*D* to 22*D* increases the FWF area by 0.002%.

The result of the optimization for the most probable wind direction (wind blowing from west to east) could be seen in Figure 8. The left side of the figure represents the OWFL, while the right side represents the slightly different targeted layout for this wind direction. When analyzing the targeted layout, we can see how the slight crosswind motions of the FOWT minimize the aerodynamic interactions inside the FWF. Finally, we repeated this step for each wind direction to achieve the targeted layouts for all wind directions. Compared with the OWFL at wind speed of 10 m/s, the FWF can produce 4.9% more energy if we achieved the targeted dynamic layout for all wind directions.

3.4 | Mooring systems full factorial design matrix

The full factorial design matrix had 419,904 different MS designs, which were created by permuting over all possible combinations of the permutable design parameters. To create the design matrix, we had to define the values of both the constant and permutable design parameters. First, we defined the values of the constant design parameters, the number of mooring lines in each MS was fixed to three lines, the water depth was kept at 200 m, and we assumed that all mooring lines were made of steel chains. For the permutable parameters we defined them as follows:

- Mooring line diameters had two possible values for each mooring line: 0.06 m and 0.12 m. Hence, we had 2^3 possible MS designs combinations.
- Line headings had 72 possible combinations; this assured that all possible mooring line headings combinations were covered, and no MS was a rotated image of another one. The minimum allowable angle between two lines was defined as 10˚.
- Anchor radii had three possible values for each mooring line 3*D*, 4*D*, and 5*D*.
- The lines length coefficient β had three possible values 0.5, 0.7, and 0.9. Therefore, the anchors radii and the lines' length lead to 9^3 possible MS designs combinations.

3.5 | Mooring systems database

After creating the full factorial design matrix, we iterated over all possible MS designs and saved the results if they satisfied the defined constraints. In this step, we used the python-based quasi-static tool Moorpy[20] to calculate the FOWT's equilibrium positions when considering the wind forces X_1 and in the absence of any external forces X_0. Moorpy calculates the mooring forces, the inertial forces of the FOWT, and the hydrostatic restoring forces on the floater and then finds the overall FOWT equilibrium position. When the wind force is included, Moorpy models it as a force vector acting directly on the FOWT at sea water level. The database was created at a wind speed of 10 m/s, and all wind directions were considered with a step size of 5°. The aerodynamic force we applied includes only the horizontal forces, and no moments are applied to the FOWT.

The MS designs were only saved in the database if they passed the user defined constraints. The main goal of these constraints was to ensure that our MS designs were as realistic as possible and could supply the required yaw stiffness for the floating platform's stability. The three constraints were as follows:

- The floater's platform yaw angle cannot exceed 10°.
- The floater's platform roll angle cannot exceed 2°.
- The maximum allowable FOWT displacement in the wind direction (ΔX_w) is 1*D*.

After we applied these constraints, only 6309 MS designs were accepted from the overall 419,904 possible MS designs in the design matrix. These designs included 19 unique combinations of the line headings from the 72 possible line headings combinations in the full factorial design matrix.

3.6 | Customized MS design

Once we calculated the targeted FWF layout at each wind direction $\Delta \boldsymbol{X}_{tr}$ and the ΔX_p from the MS database, our goal was to find a MS design to be coupled to each FOWT in the farm to increase the energy production. We followed the methods presented in Section 2.5, and we had in average around 250 possible MS designs for each FOWT in the FWF. After iterating over the MS designs of each FOWT as in Figure 5, we reached a customized MS design for each FOWT that led to the highest increase in energy production considering all wind directions. The customized MS design for each FOWT in the wind farm is presented in Table A1. The overall energy produced by the final dynamic FWF layout was 2.2% higher compared to the OWFL at 10 m/s. This means we could achieve 44.9% of our targeted energy gain from Section 3.3.

To understand why we could not fully achieve our targeted energy gain, we compare the final layout to the targeted layout for the most dominant wind direction in Figure 9. We see that the final layout does not perfectly match the targeted layout. The reason is mainly because the targeted layout looked at each wind direction separately assuming there was no correlation between the displacements at different wind directions. On the other hand, this was not the case for the final layout, as it considered the displacements the MS could achieve for every wind direction. The MS that led to the highest overall energy gain for all wind directions was chosen as in reality no MS can achieve all the targeted displacements for all wind directions. In general, we must find a compromise between the actual displacements a MS can achieve and the targeted displacements that leads to the highest total energy gain.

The other difference between the targeted and the final layout that is clear in Figure 9 is the displacement in the wind direction. In Section 3.3, to obtain the targeted dynamic FWF layout, we only allowed crosswind displacements. However, once the FOWT is attached to the MS, there is always a displacement in the wind direction, as the thrust force acts on the rotor and displaces the FOWT in the wind direction. However, all the MS in the database have a maximum displacement in the wind direction of 1*D*, and since all the FOWTs in the farm would move together into the wind direction, we believe this had limited effects on the results.

Figure 10 shows the percentage of energy gain for the targeted and the final layouts compared with the OWFL at each wind direction. For the targeted layout, we can see that the energy gain does not follow the wind rose, and the highest gain does not happen at the two most dominant wind directions. This is expected as the wind farm optimization we used to obtain the OWFL aimed to find a layout that can achieve the highest possible energy production considering all wind directions. Therefore, it is expected that the global optimum layout is highly affected by the two most dominant wind directions, so the layout is more optimized for the dominant wind directions than other wind directions. Consequently, it is harder to further optimize the FWF layout for the dominant wind directions compared with the less dominant wind directions. From this, we can also conclude that the wind rose has a big influence on the results. For example, if a site has a wind rose with many dominant wind directions, we predict that relocating the FOWT will lead to higher energy gain. On the other hand, if a site's wind rose is dominated with one wind direction, it will be less beneficial to relocate the turbines in a FWF.

For the final energy gain in Figure 10, the highest gain occurs at the most dominant wind direction, while the second highest gain happens at the wind direction with the highest targeted gain. In general, we cannot see a correlation between the final gain values at each wind direction in

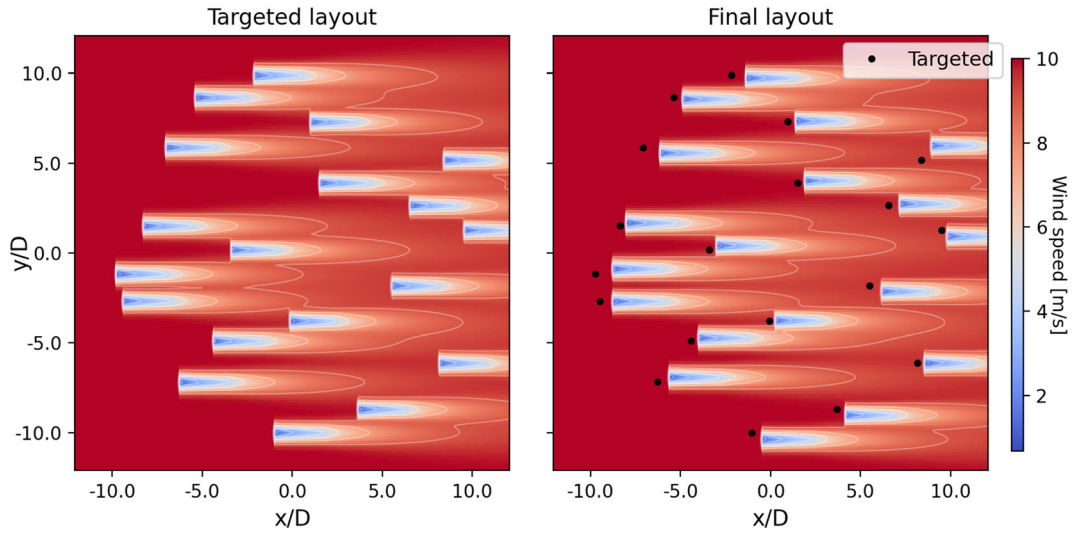

FIGURE 9 The targeted and final FWF layouts at the main wind direction at 10 m/s

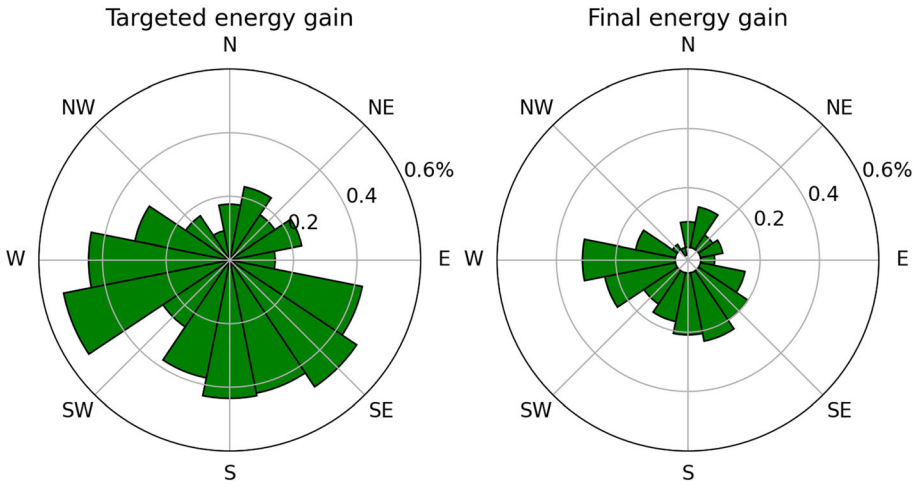

FIGURE 10 Targeted (left) and final (right) energy gains at each wind direction at constant wind speed of 10 m/s

Figure 10 and the wind rose distribution or the targeted energy gain distribution. With a system as complicated and multi-disciplinary as a FWF, it is not possible to conclude that the wind direction with the highest energy gain will always be the most dominant wind direction. This highly depends on each case study and the different parameters of the FWF considered.

3.7 | Calculate the overall AEP of the FWF with the dynamic layout

Until this point, all the calculations assumed that the wind speed is constant at 10 m/s for all wind directions within the wind rose. However, this is not a realistic assumption and overestimates the results; we will gain less energy than 2.2% if we include all wind speeds. This is due to the fact that wake effects do not affect the energy production at above rated wind speeds. Therefore, we used a Weibull distribution with a shape parameter $k = 2$ and a scale parameter $\lambda = 8$ m/s to produce the wind rose in Figure 11. Moreover, we assumed all wind directions within the wind rose had the same parameters for the Weibull distribution.

In addition, the MS database had the FOWT's displacements only at wind speed of 10 m/s. Therefore, the next step was to calculate the FOWT's displacements at each wind speed when attached to the customized MS designs. Afterwards, we calculated the AEP gain the FWF can achieve through self-adjusting their positions. The results showed that the AEP of the FWF can increase by 1.3% compared with the OWFL. This

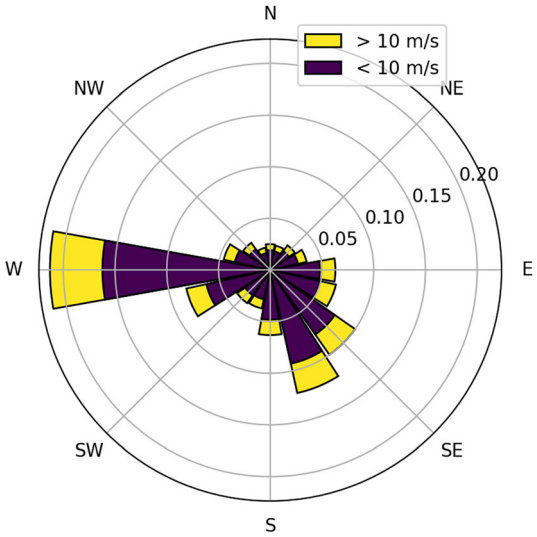

FIGURE 11 Full windrose: shape parameter $k = 2$, and a scale parameter $\lambda = 8$ m/s

increase is equivalent to 13.3 GWh annually for this case study. The Weibull distribution parameters affect the total energy gain we can achieve, as the Weibull distribution skews more toward the above rated wind speed the potential energy gain decreases and vice versa. For example, if we changed the values of the shape parameter to $k = 2.5$, and the scale parameter to $\lambda = 8$ m/s, the gain in the FWF AEP will increase to 1.6%.

4 | CONCLUSION

As we move more toward clustering wind turbines in bigger wind farms, new methods are needed to decrease the wind farms' losses. The goal of this work was to find out whether we can decrease the wake losses in a FWF by relocating the positions of FOWTs out of the wake. To answer this question, we developed a novel methodology for FWF layout design, which we presented in Section 2. As we summarized in Figure 1, the new method consists of six main steps. The first two steps are to find the targeted optimum wind farm layout for each wind direction, where we obtain a different FWF layout for each wind direction. In parallel, steps 3 and 4 aim to create a database for MS designs and the crosswind displacements that each design allow when attached to the FOWT. Afterwards, we use the targeted FWF layout and the MS designs database to find a customized MS design for each FOWT in the FWF. The goal of each customized MS design is to allow each FOWT to self-adjust its position according to the wind direction to increase the FWF's energy production. Finally, we calculate the overall gain in the FWF AEP after attaching the MS designs to each FOWT. We implemented the method as an open-source tool in python,[9] to be used and developed further within the wind energy community.

After introducing the method, we applied it in Section 3 on a general case study, to answer our research question. The results showed that allowing a self-adjusting FWF layout led to an increase in the AEP of the wind farm. The final FWF layout showed an increase in AEP between 1.6% and 1.3% when compared with a fixed position wind farm layout. We must keep in mind that the method we present here was created only to find out if there is a benefit in a self-adjusting floating layout. Enhancing this novel method further will lead to a bigger increase in the AEP of the FWF. Therefore, we can conclude from the work done within this paper that allowing a FWF to self-adjust its layout according to the wind speed and wind direction is a very promising idea with high potential. Although we answered our research question in this paper and showed that a self-adjusting FWF layout is beneficial for the FWF's AEP, it represents a first step to build on in future research.

In the following steps we would like to do a sensitivity analysis to check the effect of having a wind rose with different wind directions distributions on the self-adjusting FWF in AEP. For example, we want to use a wind farm with multiple dominant wind directions, and with a mono-directional wind farm. Additionally, we want to study the effect of having a bigger wind farm with more turbines, and with different regular and irregular boundary shapes for the baseline wind farm layout. This sensitivity analysis will show us the conditions where it is the most beneficial to use a self-adjusting wind farm layout.

Additionally, in the future, we want to increase the fidelity of our analysis and include dynamic simulations, to study the dynamic responses of the self-adjusting FWF layout. We want to verify that the FWF will react according to our expectations in dynamic simulations, with turbulent wind fields and stochastic waves. In addition, the dynamic loads acting on the customized MS design attached to each FOWT in the FWF shall be analyzed. We are planning to check if the MS designs can pass the ultimate limit state (ULS) and the fatigue limit state (FLS) for operation and extreme loading conditions. Furthermore, we will analyze the limitations the dynamic cable introduces on the FOWT motions.

In this work, we were able to present an innovative approach for FWF wind farm design, which can decrease the wake losses inside the farm and increase its energy production. The approach aimed at including the MS design as part of the FWF layout design procedure, where each FOWT had a customized MS design to self-adjust the FOWT's position according to the wind direction and the wind speed. Applying this approach showed that a self-adjusting FWF layout can increase the AEP up to 1.6%, when compared with the current state of the art wind farm layout optimization.

ACKNOWLEDGEMENT

The research leading to these results has received funding from the European Union's Horizon 2020 research and innovation program under grant agreement no. 815083 (COREWIND). Open Access funding enabled and organized by Projekt DEAL.

PEER REVIEW

The peer review history for this article is available at https://publons.com/publon/10.1002/we.2797.

ORCID


Mohammad Youssef Mahfouz https://orcid.org/0000-0002-3057-270X

REFERENCES

1. Vermeer LJ, Sørensen JN, Crespo A. Wind turbine wake aerodynamics. *Progress Aerosp Sci*. 2003;39(6-7):467-510.
2. Porté-Agel F, Bastankhah M, Shamsoddin S. *Wind-Turbine and Wind-Farm Flows: A Review*, Vol. 174. Netherlands: Springer; 2020. https://doi.org/10.1007/s10546-019-00473-0
3. Fleming PA, Ning A, Gebraad PMO, Dykes K. Wind plant system engineering through optimization of layout and yaw control. *Wind Energy*. 2016;19(2):329-344. https://doi.org/10.1002/we.1836
4. Perez-Moreno SS, Dykes K, Merz KO, Zaaijer MB. Multidisciplinary design analysis and optimisation of a reference offshore wind plant. *J Phys: Conf Ser*. 2018;1037(4):42004.
5. Fleming P, Gebraad PMO, Lee S, et al. Simulation comparison of wake mitigation control strategies for a two-turbine case. *Wind Energy*. 2015;18(12):2135-2143. https://onlinelibrary.wiley.com/doi/10.1002/we.1810
6. Kheirabadi AC, Nagamune R. Modeling and power optimization of floating offshore wind farms with yaw and induction-based turbine repositioning. *Proc Am Control Conf*. 2019;2019:5458-5463.
7. Kheirabadi AC, Nagamune R. Real-time relocation of floating offshore wind turbine platforms for wind farm efficiency maximization: An assessment of feasibility and steady-state potential. *Ocean Eng*. 2020;208:107445. https://doi.org/10.1016/j.oceaneng.2020.107445
8. Rodrigues SF, Teixeira Pinto R, Soleimanzadeh M, Bosman PAN, Bauer P. Wake losses optimization of offshore wind farms with moveable floating wind turbines. *Energy Conv Manag*. 2015;89:933-941. https://doi.org/10.1016/j.enconman.2014.11.005
9. Mahfouz MY. *Swe-unistuttgart/floatingways: Beta version*: Zenodo; 2022. https://doi.org/10.5281/zenodo.7071666
10. Mahfouz MY, Hall M, Cheng PW. A parametric study of the mooring system design parameters to reduce wake losses in a floating wind farm. *J Phy: Conf Ser*. 2022;2265(4):42004. https://iopscience.iop.org/article/10.1088/1742-6596/2265/4/042004
11. NREL. *Floris. version 2.4*: GitHub; 2021. https://github.com/NREL/floris
12. Wu N, Kenway G, Mader CA, Jasa J, Martins JRRA. pyoptsparse: a python framework for large-scale constrained nonlinear optimization of sparse systems. *J Open Source Softw*. 2020;5(54):2564.
13. Baker NF, Stanley APJ, Thomas JJ, Ning A, Dykes K. Best practices for wake model and optimization algorithm selection in wind farm layout optimization. In: AIAA Scitech 2019 Forum; 2019:540.
14. Thomas JJ, McOmber S, Ning A. Wake expansion continuation: multi-modality reduction in the wind farm layout optimization problem. *Wind Energy*. 2022;25(4):678-699.
15. Mahfouz MY, Molins C, Trubat P, et al. Response of the International Energy Agency (IEA) Wind 15 MW WindCrete and Activefloat floating wind turbines to wind and second-order waves. *Wind Energy Sci*. 2021;6(3):867-873.
16. Abkar M, Porté-Agel F. Influence of atmospheric stability on wind-turbine wakes: a large-eddy simulation study. *Phys Fluids*. 2015;27(3):35104. https://doi.org/10.1063/1.4913695
17. Bastankhah M, Porté-Agel F. A new analytical model for wind-turbine wakes. *Renew Energy*. 2014;70:116-123. https://doi.org/10.1016/j.renene.2014.01.002
18. Crespo A, Hernández J. Turbulence characteristics in wind-turbine wakes. *J Wind Eng Industr Aerodyn*. 1996;61(1):71-85.
19. Gill PE, Murray W, Saunders MA. SNOPT: An SQP algorithm for large-scale constrained optimization. *SIAM Rev*. 2005;47(1):99-131.
20. Hall M, Housner S, Sirnivas S, Wilson S. *Moorpy (quasi-static mooring analysis in python)*: GitHub; 2021. https://doi.org/10.11578/dc.20210726.1

How to cite this article: Mahfouz MY, Cheng P-W. A passively self-adjusting floating wind farm layout to increase the annual energy production. *Wind Energy*. 2022;1-15. doi:10.1002/we.2797

APPENDIX A

TABLE A1 Customized MS design

Turbines	Line 1				Line2				Line 3			
-	Heading (°)	Diameter (m)	Anchor radius (m)	Length (m)	Heading (°)	Diameter (m)	Anchor radius (m)	Length (m)	Heading (°)	Diameter (m)	Anchor radius (m)	Length (m)
0	215	0.06	1200	1266.1	355	0.12	720	826.17	105	0.06	1200	1266.1
1	230	0.06	1200	1266.1	0	0.06	1200	1302.66	140	0.12	960	1028.25
2	35	0.12	720	791.95	175	0.06	1200	1266.1	285	0.12	960	1063.95
3	70	0.06	1200	1339.22	190	0.06	1200	1266.1	310	0.12	960	1063.95
4	85	0.06	1200	1266.1	205	0.12	720	791.95	345	0.12	720	791.95
5	165	0.06	1200	1302.66	285	0.12	720	860.39	55	0.12	720	860.39
6	330	0.06	1200	1266.1	90	0.12	720	860.39	230	0.12	960	1028.25
7	45	0.12	720	791.95	175	0.12	720	791.95	335	0.12	720	791.95
8	155	0.12	720	791.95	315	0.12	720	791.95	45	0.12	1200	1266.1
9	0	0.12	720	791.95	140	0.12	720	791.95	250	0.12	960	1028.25
10	10	0.12	1200	1339.22	140	0.12	1200	1266.1	270	0.06	1200	1302.66
11	55	0.12	1200	1266.1	175	0.06	1200	1266.1	315	0.06	1200	1339.22
12	60	0.12	720	791.95	180	0.12	720	791.95	320	0.06	1200	1266.1
13	225	0.12	960	1099.65	345	0.06	1200	1339.22	105	0.12	960	1063.95
14	60	0.06	1200	1266.1	190	0.12	1200	1266.1	340	0.12	720	791.95
15	150	0.06	1200	1302.66	300	0.12	960	1028.25	40	0.12	1200	1266.1
16	55	0.12	720	791.95	185	0.06	1200	1266.1	315	0.12	960	1028.25
17	45	0.12	720	860.39	185	0.12	720	791.95	295	0.12	1200	1266.1
18	45	0.12	720	826.17	185	0.12	720	791.95	295	0.06	1200	1302.66